Measurement of the $WW\gamma$ vertex through single photon production at e^+e^- colliders

Gilles Couture*

Département de Physique, Université du Québec à Montréal, C.P. 8888, Succ. Centre-Ville, Montréal, Québec, Canada H3C 3P8

Stephen Godfrey†

Ottawa-Carleton Institute for Physics, Department of Physics, Carleton University, Ottawa, Canada K1S 5B6

We perform a detailed study of the process $e^+e^- \to \gamma\nu_l\bar{\nu}_l$ and its sensitivity to anomalous gauge boson couplings of the γWW vertex. We concentrate on CERN LEP II energies, $\sqrt{s} = 200$ GeV, and energies appropriate to the proposed Next Linear Collider (NLC), a high energy e^+e^- collider, with center of mass energies $\sqrt{s} = 500$ and 1 TeV. At 200 GeV, the process offers, at best, a consistency check of other processes being considered at LEP 200. At 500 GeV, the parameters κ_γ and λ_γ can be measured to about ± 0.05 and ± 0.1, respectively, at 95% C.L. while at 1 TeV, they can be measured to about ± 0.02. At the high luminosities anticipated at high energy linear colliders precision measurements are likely to be limited by systematic rather than statistical errors.

PACS number(s): 13.10.+q, 12.15.Ji, 14.70.Bh, 14.70.Fm

I. INTRODUCTION

The major preoccupation of particle physics is the search for physics beyond the standard model, or equivalently, for deviations from standard model predictions. To this end, measurements at the CERN e^+e^- collider LEP 100 and the SLAC Linear Collider (SLC) [1] have provided stringent tests [2, 3] of the standard model of the electroweak interactions [4]. However, it is mainly the fermion–gauge-boson couplings that have been tested and the gauge sector of the standard model remains poorly constrained. A stringent test of the gauge structure of the standard model is provided by the trilinear gauge vertices (TGV's); the γWW and ZWW vertices. Within the standard model, these couplings are uniquely determined by $SU(2)_L \times U(1)$ gauge symmetry so that a precise measurement of the vertex poses a severe test of the gauge structure of the theory. If these couplings were observed to have different values than their standard model values, it would indicate the need for physics beyond the standard model.

The study of the trilinear gauge boson couplings by studying W pair production is one of the primary motivations for the LEP 200 upgrade [5–7] in which a precision of 30–40 % is expected from cross section and W angular distribution measurements. In the far future there is growing interest in the physics that can be done at high energy e^+e^- colliders with $\sqrt{s} = 500$ GeV or $\sqrt{s} = 1$ TeV, referred to as the Next Linear Collider (NLC), the Japan Linear Collider (JLC), or the CERN Linear Collider (CLIC) [8–13]. Various options are being studied including $e\gamma$ and $\gamma\gamma$ collisions where the energetic photons are obtained by backscattering a laser on one of the incident leptons. Measurements at these colliders are very sensitive to anomalous couplings with $e\gamma$ and $\gamma\gamma$

collisions putting some of the more stringent bounds on anomalous $WW\gamma$ couplings [14–16].

A problem common to many processes used to study TGV's is that they involve both the $WW\gamma$ and WWZ vertices, making it difficult to disentangle the contributions. In a previous paper we presented a detailed study of the process $e^+e^- \to \nu_l\bar{\nu}_l\mu^+\mu^-$ motivated by our interest in isolating the WWZ and $WW\gamma$ vertices by appropriate kinematic cuts on the invariant mass of the $\mu^+\mu^-$ [17]. Included in this final state are contributions from the underlying process $e^+e^- \to \nu_l\bar{\nu}_l\gamma^* \to \nu_l\bar{\nu}_l\mu^+\mu^-$ which shows up most dramatically when $M_{\mu^+\mu^-} \to 0$. However, because of the muons' masses it does not quite isolate the process in which we are interested. In this paper we take the obvious limit and study the sensitivity of the process $e^+e^- \to \gamma\nu_l\bar{\nu}_l$ to anomalous $WW\gamma$ couplings [9, 18]. This process has also been used as a means of counting the number of light neutrino species [19].

To parametrize the $WW\gamma$ vertex we use the most general parametrization possible that respects Lorentz invariance, electromagnetic gauge invariance and CP invariance [5, 20, 21] since it has become the standard parametrization used in phenomenology and therefore makes the comparison of the sensitivity of different measurements to the TGV's straightforward. We do not consider CP-violating operators in this paper as they are tightly constrained by measurement of the neutron electron dipole moment which constrains the two CP-violating parameters to $|\tilde{\kappa}_\gamma|, |\tilde{\lambda}_\gamma| \lesssim 10^{-4}$ [22]. Therefore the $WW\gamma$ vertex has two free independent parameters, κ_γ and λ_γ and is given by [5, 20]

$$\mathcal{L}_{WW\gamma} = -ie\left\{ (W^\dagger_{\mu\nu}W^\mu A^\nu - W^\dagger_\mu A_\nu W^{\mu\nu}) \right.$$
$$\left. + \kappa_\gamma W^\dagger_\mu W_\nu F^{\mu\nu} - \frac{\lambda_\gamma}{M_W^2} W^\dagger_{\lambda\mu} W^\mu_\nu F^{\nu\lambda} \right\}, \quad (1)$$

where A^μ and W^μ represent the photon and W^- fields,

*Electronic address: couture@osiris.phy.uqam.ca
†Electronic address: godfrey@physics.carleton.ca

respectively, $W_{\mu\nu} = \partial_\mu W_\nu - \partial_\nu W_\mu$ and $F_{\mu\nu} = \partial_\mu A_\nu - \partial_\nu A_\mu$ and M_W is the W boson mass. Higher dimension operators would correspond to momentum dependence in the form factors which we ignore. At the tree level the standard model requires $\kappa_\gamma = 1$ and $\lambda_\gamma = 0$. Note that the presence of the W-boson mass factor in the λ_V term is ad hoc and one could argue that the scale Λ of new physics would be more appropriate. We will conform to the usual parametrization and will not address this issue any further.

We studied the sensitivity of this process at KEK TRISTAN and LEP and/or SLC energies where there exist data [23, 24] that we could in principle use to bound the $WW\gamma$ couplings. However, we found that the process was insufficiently sensitive at these energies to put meaningful bounds on the $WW\gamma$ coupling with the integrated luminosities already accumulated or expected in the foreseeable future. We therefore start with $\sqrt{s} = 200$ GeV appropriate to LEP 200 since this machine will be operational in the relatively near future [6]. We then turn to the proposed JLC, NLC, or CLIC e^+e^- colliders with possible center of mass energies of $\sqrt{s} = 500$ GeV and 1 TeV [10–13]. We do not include any beamsstrahlung radiation effects in our calculation [25]. These effects are very much machine dependent (beam intensity, bunch geometry, etc.) and known to be negligible at 200 GeV, and small at 500 GeV. However, although they can be quite important at 1000 GeV, there has been progress in strategies to minimize the effects of beamstrahlung radiation.

II. CALCULATIONS AND RESULTS

The diagrams contributing to the process $e^+e^- \rightarrow \gamma\nu_l\bar{\nu}_l$ are shown in Fig. 1. The main advantage of this process is that it depends only on the $WW\gamma$ vertex. In addition, our signal [Fig. 1(a)] should increase with energy, for two reasons: it is a t-channel process and will not decrease with energy as do the other contributions to the total process, especially when suitable kinematic cuts are imposed to eliminate the on-shell Z contribution [Figs. 1(d) and 1(e)]. Also, anomalous couplings, in general, become more important at higher energies.

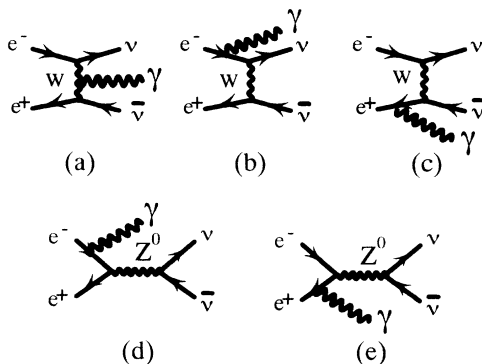To evaluate the cross sections and different distribu-

FIG. 1. The Feynman diagrams contributing to the process $e^+e^- \rightarrow \gamma\nu\bar{\nu}$.

tions, we used the CALKUL helicity amplitude technique [26] to obtain expressions for the matrix elements and performed the phase space integration using Monte Carlo techniques [27]. The expressions for the helicity amplitudes are lengthy and unilluminating so we do not include them here. The interested reader can obtain them directly from the authors. To obtain numerical results we used the values $\alpha = 1/128$, $\sin^2\theta = 0.23$, $M_Z = 91.187$ GeV, $\Gamma_Z = 2.5$ GeV, $M_W = 80.2$ GeV, and $\Gamma_W = 2.1$ GeV.

The signal we are studying is an energetic γ plus missing transverse momentum. The largest potential background is Bhabha scattering with a hard photon and the electron and positron going down the beam pipe. This should not be a serious problem given that we are interested in energetic photons and the luminosity monitors, based on Bhabha scattering, should be able to veto any such events. In order to take into account finite detector acceptance, we require that the photon be at least $10°$ away from the beam line although in practice the cuts we use to enhance the signal are much more restrictive than this (typically $\sim 30°$).

In principle we should include QED radiative corrections from soft photon emission and the backgrounds due to a second photon either that is lost down the beam pipe or collinear to the hard photon being measured and therefore unresolved [28]. Although soft photon emission can reduce the cross section substantially, its inclusion does not substantially affect the bounds we obtain and therefore our conclusions. The effects of an unseen second photon turn out to be quite small. Since both these contributions depend on details of detector such as energy resolution and do not alter our conclusions we leave them out but stress that they must be included in detailed detector Monte Carlo simulations.

The approach we followed was to examine various kinematic distributions, $d\sigma/d\cos\theta_\gamma$, $d\sigma/dE_\gamma$, $d\sigma/dE_{T_\gamma}$, and kinematic cuts to find which ones optimized the sensitivity to anomalous couplings. In general, the tightest constraints were obtained by imposing cuts on the photon energy which eliminated contributions from on-shell Z^0 production [Figs. 1(d) and 1(e)].

A. $\sqrt{s} = 200$ GeV

In Fig. 2 we show the E_γ distribution for $\sqrt{s} = 200$ GeV for several values of κ_γ and λ_γ. The most prominent feature of the distribution comes from the contribution of the on-shell Z^0 [Figs. 1(d) and 1(e)]. From Fig. 2 it can be seen that the regions off the Z^0 resonance are most sensitive to anomalous couplings with the greatest sensitivity in the region above the Z^0 resonance. This is because that region probes the largest momentum transfer through the W-boson t-channel propagators. We found that the tightest constraints could be obtained by imposing an angular cut of $35° < \theta_\gamma < 145°$ and on the two regions of E_γ: 25 GeV$< E_\gamma <$65 GeV and $E_\gamma >$88 GeV. For 25 GeV$< E_\gamma <$65 GeV the cross section is 0.14 pb which for an integrated luminosity of 500 pb^{-1} results in about a 12% statistical error. Similarly for $E_\gamma >$88 GeV $\sigma = 0.087$ pb, which gives a 50% statistical error. Monte
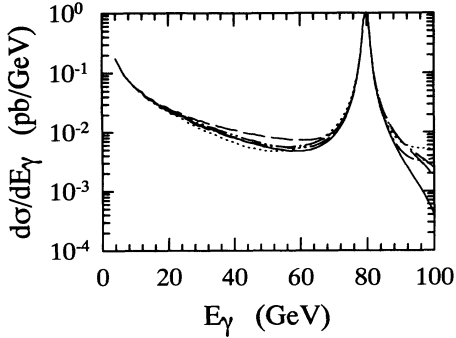
FIG. 2. The photon energy distribution, $d\sigma/dE_\gamma$ at $\sqrt{s} = 200$ GeV. The solid line is for standard model values of κ_γ and λ_γ, the long dashed line is for $\kappa_\gamma = -3$ and $\lambda_\gamma = 0$; the dotted line is for $\kappa_\gamma = 5$ and $\lambda_\gamma = 0$; the dot-dashed line is for $\kappa_\gamma = 1$ and $\lambda_\gamma = -4$; and the dot-dot-dashed line is for $\kappa_\gamma = 1.0$ and $\lambda_\gamma = 4$.

Carlo studies of SLD-type detectors give very crude estimates of systematic errors of 5% for cross section measurements [29]. Therefore the effects of including a 5% systematic error are not particularly important. The 68% C.L., 90% C.L., and 95% C.L. bounds that could be obtained with these cuts for $\sqrt{s} = 200$ GeV and integrated luminosity of $L = 500$ pb^{-1} are shown in Fig. 3 with numerical values when varying one parameter at a time given in Table I. It is worth mentioning that the *most efficient* energy and angular cuts will vary slightly with the domain of κ_γ and λ_γ being probed. However, this dependence is mild and the limits will not vary much if one uses a fixed set of cuts.
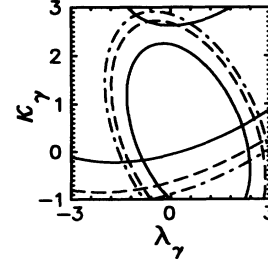

FIG. 3. Sensitivities of the TGV's to anomalous couplings for $\sqrt{s} = 200$ GeV and $L = 500$ pb^{-1}. The horizontal curves are based on $25 < E_\gamma < 65$ GeV and the vertically aligned oblongs are based on $E_\gamma > 88$ GeV. In both cases the solid curves represent 68% C.L. limits, the dashed curves 90% C.L. limits and the dot-dashed curves 95% C.L. limits.

An important question for LEP 200 is the effect on the *physics reach* of different center of mass energies. To gauge the change of the sensitivity to the TGV's for different energies we plot in Fig. 4 the 90% C.L. for $\sqrt{s} = 175$ GeV, 200 GeV, and 230 GeV. Clearly, the higher the energy the tighter the constraints that can be obtained. Roughly speaking, increasing the c.m. energy by 15% will increase the sensitivity to anomalous couplings by 30%. However, even for the highest possible energies at LEP 200 of $\sqrt{s} = 230$ GeV the obtainable bounds are not competitive with the W-pair production process or for that matter with bounds obtained by the Tevatron experiments via associated $W\gamma$ production, and will, at best, be a consistency check of other measurements.

TABLE I. Sensitivities to κ_γ and λ_γ at 95% C.L. from the process $e^+e^- \to \gamma\nu\bar{\nu}$ at a 200 GeV, 500 GeV, and 1 TeV e^+e^- colliders. The statistical error is based on the specified integrated luminosity. The entry - - - denotes a bound too weak to be relevant.

Observable		$\sqrt{s} = 200$ GeV $\delta_1^{stat}(L{=}250$ pb$^{-1})$	$\delta_2^{stat}(L{=}500$ pb$^{-1})$
$25 < E_\gamma < 65$ GeV	$\delta\kappa_\gamma$	- - -	- - -
$E_\gamma > 88$ GeV	$\delta\kappa_\gamma$	$^{-2.5}_{+2.3}$	$^{-1.9}_{+1.9}$
	$\delta\lambda_\gamma$	$^{-3.2}_{+2.9}$	$^{-2.6}_{+2.5}$
$E_{T\gamma} > 84$ GeV	$\delta\kappa_\gamma$	$^{-2.4}_{+2.9}$	$^{-2.0}_{+2.5}$
	$\delta\lambda_\gamma$	$^{-3.3}_{+2.8}$	$^{-2.8}_{+2.4}$
		-2.4	-1.9

Observable		$\sqrt{s} = 500$ GeV $\delta_1^{stat}(L{=}10$ fb$^{-1})$	$\delta_2^{stat}(L{=}50$ fb$^{-1})$
$50 < E_\gamma < 160$ GeV	$\delta\kappa_\gamma$	$^{+0.13}_{-0.12}$	$^{+0.055}_{-0.055}$
$177 < E_\gamma < 237$ GeV	$\delta\kappa_\gamma$	$^{+0.16}_{\ \ - - -}$	$^{+0.08}_{-0.10}$
	$\delta\lambda_\gamma$	$^{+0.16}_{-0.10}$	$^{+0.12}_{-0.06}$
$E_\gamma > 245$ GeV	$\delta\lambda_\gamma$	$^{+0.17}_{-0.23}$	$^{+0.10}_{-0.17}$

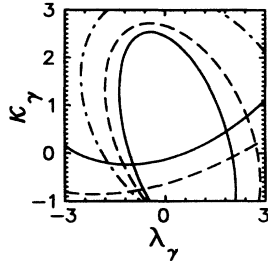| Observable		$\sqrt{s} = 1000$ GeV $\delta_1^{stat}(L{=}50$ fb$^{-1})$	$\delta_2^{stat}(L{=}200$ fb$^{-1})$
$60 < E_\gamma < 220$ GeV	$\delta\kappa_\gamma$	$^{+0.037}_{-0.036}$	$^{+0.018}_{-0.018}$
$245 < E_\gamma < 490$ GeV	$\delta\lambda_\gamma$	$^{+0.039}_{-0.015}$	$^{+0.034}_{-0.009}$

FIG. 4. Sensitivities of the TGV's to anomalous couplings at 90% C.L. for $\sqrt{s} = 230$ GeV (solid curves), $\sqrt{s} = 200$ GeV (dashed curves), and $\sqrt{s} = 175$ GeV (dot-dashed curves) all for 500 pb^{-1} integrated luminosity. The horizontal curves are based on $25 < E_\gamma < 80$ GeV for $\sqrt{s} = 230$ GeV, and $25 < E_\gamma < 65$ GeV for $\sqrt{s} = 200$ GeV, while the vertical oblongs are based on $E_\gamma > 104$ GeV for $\sqrt{s} = 230$ GeV, $E_\gamma > 88$ GeV for $\sqrt{s} = 200$ GeV, and $E_\gamma > 72$ GeV for $\sqrt{s} = 175$ GeV.

B. $\sqrt{s} = 500$ GeV

We next turn to an "NLC"-type e^+e^- collider with $\sqrt{s} = 500$ GeV. We consider integrated luminosities of 10 and 50 fb^{-1}. The photon energy distributions for several values of κ_γ and λ_γ are shown in Fig. 5. As before, the values of E_γ most sensitive to anomalous couplings are off the Z^0 resonance and κ_γ and λ_γ are sensitive to different values of E_γ. For example, κ_γ is most sensitive to $50 < E_\gamma < 160$ GeV while λ_γ is most sensitive to $177 < E_\gamma < 237$ GeV. The bounds obtained from these observables are shown in Fig. 6 with numerical values obtained by varying one parameter at a time given in Table I. One could obtain additional information by using the transverse energy distribution of the photons with and without left-handed polarized electrons. For $50 < E_\gamma < 160$ GeV the cross section
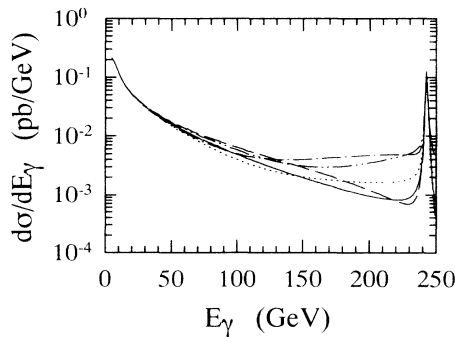

FIG. 6. Sensitivities of the TGV's to anomalous couplings for $\sqrt{s} = 500$ GeV and $L=50$ fb^{-1}. The horizontal curves are based on $50 < E_\gamma < 160$ GeV; the vertical curves are based on $E_\gamma > 245$ GeV; and the upside-down U shaped curves are based on $177 < E_\gamma < 237$ GeV. In all cases the solid lines are 68% C.L. and the dot-dashed curves are 95% C.L.

is $\sigma = 0.27$ pb which for an integrated luminosity of 50 fb^{-1} gives a statistical error of 0.8%. Likewise for $177 < E_\gamma < 237$ GeV we obtain $\sigma = 0.024$ pb and $\delta\sigma^{\text{stat}}/\sigma = 3\%$ and for $E_\gamma > 245$ GeV $\sigma = 0.0019$ pb and $\delta\sigma^{\text{stat}}/\sigma = 10\%$. Given the small statistical errors including a 5% systematic error will have a considerable effect on the bounds that can be obtained. For example for $50 < E_\gamma < 160$ GeV, where the statistical error is smallest including a 5% systematic error reduces the sensitivity by roughly a factor of 5 while for $177 < E_\gamma < 237$ GeV where the statistical error is larger it has only a small effect and for $E_\gamma > 245$ GeV where the statistical error is largest the effect of the systematic error is neglegible.

C. $\sqrt{s} = 1$ TeV

The final case we consider is a 1 TeV e^+e^- collider. In Fig. 7 we show the photon energy distribution for several values of κ_γ and λ_γ. As in the 500 GeV case we find that κ_γ and λ_γ are sensitive to different values of E_γ.

FIG. 5. The photon energy distribution, $d\sigma/dE_\gamma$ for $\sqrt{s} = 500$ GeV. The solid line is for standard model values of κ_γ and λ_γ, the long dashed line is for $\kappa_\gamma = 0.0$ and $\lambda_\gamma = 0$; the dotted line is for $\kappa_\gamma = 2.0$ and $\lambda_\gamma = 0$; the dot-dashed line is for $\kappa_\gamma = 1$ and $\lambda_\gamma = -1.0$; and the dot-dot-dashed line is for $\kappa_\gamma = 1.0$ and $\lambda_\gamma = 1.0$.
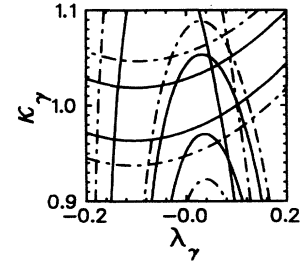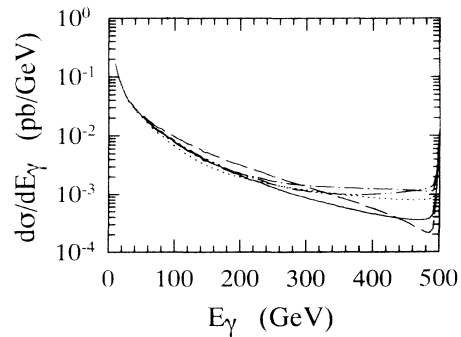

FIG. 7. The photon energy distribution, $d\sigma/dE_\gamma$ for $\sqrt{s} = 1000$ GeV. The solid line is for standard model values of κ_γ and λ_γ, the long dashed line is for $\kappa_\gamma = 0.2$ and $\lambda_\gamma = 0$; the dotted line is for $\kappa_\gamma = 1.8$ and $\lambda_\gamma = 0$; the dot-dashed line is for $\kappa_\gamma = 1$ and $\lambda_\gamma = -0.2$; and the dot-dot-dashed line is for $\kappa_\gamma = 1.0$ and $\lambda_\gamma = 0.2$.
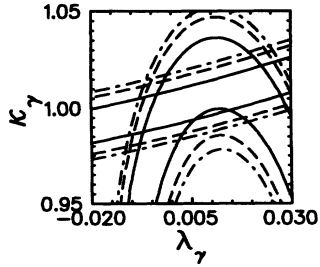
FIG. 8. Sensitivities of the TGV's to anomalous couplings for $\sqrt{s} = 1$ TeV and $L=200$ fb^{-1}. The horizontal curves are based on $60 < E_\gamma < 220$ GeV; and the inverted U shaped curves are based on $245 < E_\gamma < 490$ GeV. In both cases the solid lines are 68% C.L., the dashed lines are 90% C.L., and the dot-dashed curves are 95% C.L.

III. CONCLUSIONS

We have examined the usefulness of the process $e^+e^- \rightarrow \gamma\nu_l\bar{\nu}_l$ for measuring the γW^+W^- vertex. The sensitivity of this process to anomalous coupling is greatly enhanced (by a factor of 5–8 generally) by eliminating the on-shell Z and by splitting the energy domain of the photon into more than one bin. The process turned out to be too insensitive at TRISTAN and LEP-100 and/or SLC energies to obtain bounds competitive with recent results from the Fermilab Tevatron. In fact, the same is also true for LEP-200 energies which at best will offer a consistency check of bounds extracted from W-pair production at LEP-200 and the Tevatron. At higher energy e^+e^- colliders, this process can lead to very stringent bounds, precise enough to test the TGV's at the level of radiative corrections. We used the high luminosities planned for at the high energy e^+e^- colliders to estimate statistical errors. When we included reasonable estimates of systematic errors we found that the limiting factor in high precision measurements will likely be systematic errors not statistical errors. However, we based our analysis on optimizing cuts on E_γ and $E_{T\gamma}$ and it is likely that performing a more detailed maximum likelihood fit of real data would make fuller use of the information in the data thereby obtaining tighter bounds. The challenge will be to reduce the systematic errors and one should be very careful with respect to the conclusions one makes by considering only statistical errors.

For the photon energy range $60 < E_\gamma < 220$ GeV, $\sigma = 0.39$ pb which for an integrated luminosity of 200 fb^{-1} gives $\delta\sigma^{\text{stat}}/\sigma = 0.3\%$ while for $245 < E_\gamma < 490$ GeV $\sigma = 0.05$ pb $\delta\sigma^{\text{stat}}/\sigma = 1\%$. Including a 5% systematic error weakens the bounds on the TGV's considerably, even more so at $\sqrt{s} = 1$ TeV than at 500 GeV.

In Fig. 8 we show the bounds that could be obtained using $60 < E_\gamma < 220$ GeV and $245 < E_\gamma < 490$ GeV and give some numerical values in Table I. The bounds obtainable on κ_γ are down to the percent level necessary to probe radiative corrections to the gauge boson vertices. Although the bounds on λ_γ are also down to this level radiative corrections are about an order of magnitude smaller so that it is unlikely that deviations from the tree-level value could be observed unless there was a radical departure from the standard model by, for example, compositeness.

[1] M. Swartz, in *Lepton and Photon Interactions,* Proceedings of the XVI International Symposium, Ithaca, New York, 1993, edited by P. Drell and D. Rubin, AIP Conf. Proc. No. 302 (AIP, New York, 1994).

[2] W. Hollik, in *Lepton and Photon Interactions* [1].

[3] C.P. Burgess, S. Godfrey, H. König, D. London, and I. Maksymyk, Phys. Rev. D **49**, 6115 (1994).

[4] S.L. Glashow, Nucl. Phys. **22**, 579 (1961); S. Weinberg, Phys. Rev. Lett. **19**, 1264 (1967); A. Salam, in *Elementary Particle Theory: Relativistic Groups and Analyticity (Nobel Symposium No. 8),* edited by N. Svartholm (Almqvist and Wiksell, Stockholm, 1968).

[5] K. Hagiwara *et al.*, Nucl. Phys. **B282**, 253 (1987).

[6] D. Zeppenfeld, Phys. Lett. B **183**, 380 (1987); D. Treille *et al.*, in *Proceedings of the ECFA Workshop on LEP 200,* Aachen, Germany, 1986, edited by A. Böhm and W. Hoogland (CERN Report No. 87-08, Geneva, Switzerland, 1987), Vol. 2, p. 414; D.A. Dicus and K. Kallianpur, Phys. Rev. D **32**, 35 (1985); M.J. Duncan and G.L. Kane, Phys. Rev. Lett. **55**, 773 (1985); E.N. Argyres and C.G. Papadopoulos, Phys. Lett. B **263**, 298 (1991).

[7] G. Kane, J. Vidal, and C.P. Yuan, Phys. Rev. D **39**, 2617 (1990), and references therein.

[8] D. Treille, in *Proceedings of the Workshop on Physics and Experiments with Linear e^+e^- Colliders,* Waikoloa, Hawaii, 1993, edited by F. Harris (World Scientific, Singapore, 1994); A. Djouadi and P.M. Zerwas, in *Proceedings of Beyond the Standard Model III,* edited by S. Godfrey and P. Kalyniak, Ottawa, Canada, 1992 (World Scientific, Singapore, 1993), p. 204.

[9] A. Miyamoto, in *Proceedings of the Workshop on Physics and Experiments with Linear e^+e^- Colliders* [8], p. 141.

[10] See, for example, B. Wiik, in *Proceedings of the Workshop on Physics and Experiments with Linear e^+e^- Colliders* [8].

[11] *Proceedings of the First Workshop on Japan Linear Collider (JLC),* Tsukuba, Japan, 1989, edited by S. Kawabata (KEK Report No. 90-2, Tsukuba, 1990); *Proceedings of the Second Workshop on Japan Linear Collider,* Tsukuba, Japan, 1990, edited by S. Kawabata (KEK Report No. 91-10, Tsukuba, 1991).

[12] C. Ahn *et al.*, "Opportunities and Requirments for Ex-

perimentation at a Very High Energy e^+e^- Collider,"
SLAC Report No. SLAC-0329, 1988 (unpublished).

[13] Proceedings of the Workshop on Physics at Future Accelerators, CERN Yellow Report No. 87-07, 1987 (unpublished).

[14] E. Yehudai, Phys. Rev. D **41**, 33 (1990); **44**, 3434 (1991); S. Godfrey and A.K. Peterson, Carleton University Report No. OCIP/C-92-7 (unpublished).

[15] G. Couture, S. Godfrey, and P. Kalyniak, Phys. Rev. D **39**, 3239 (1989); **42**, 1841 (1990); Phys. Lett. B **218**, 361 (1989) and references therein.

[16] S.Y. Choi and F. Schrempp, Phys. Lett. B **272**, 149 (1991); G. Bélanger and G. Couture, Phys. Rev. D **49**, 5720 (1994).

[17] G. Couture, S. Godfrey, and R. Lewis, Phys. Rev. D **45**, 777 (1992); G. Couture and S. Godfrey, ibid. **49**, 5709 (1994).

[18] G.V. Borisov, V.N. Larin, and F.F. Tikhonin, Z. Phys. C **41**, 287 (1988).

[19] H. Band et al., in Proceedings of the Second Symposium on the Fourth Family of Quarks and Leptons, Santa Monica, California, 1989, edited by D. Cline and A. Soni (N.Y. Academy of Sciences, New York, 1989); J.D. Ware and M.E. Machacek, Phys. Lett. **147B**, 415 (1984); G. Couture and J.N. Ng, Phys. Rev. D **34**, 744 (1986).

[20] K. Gaemers and G. Gounaris, Z. Phys. C **1**, 259 (1979).

[21] K.-i Hikasa, Phys. Rev. D **33**, 3203 (1986); K. Hagiwara et al., Nucl. Phys. **B282**, 253 (1987); J. Fleischer et al.,

[22] W.J. Marciano and A. Queijeiro, Phys. Rev. D **33**, 3449 (1986); F. Boudjema, K. Hagiwara, C. Hamzaoui, and K. Numata, ibid. **43**, 2223 (1991).

[23] VENUS Collaboration, N. Hosoda et al., KEK Report No. 93-194, 1994 (unpublished).

[24] OPAL Collaboration, M.Z. Akrawy et al., Z. Phys. C **50**, 373 (1991); L3 Collaboration, B. Adeva et al., Phys. Lett. B **275**, 209 (1992); **297**, 468 (1992); Aleph Collaboration, D. Buskulic et al., ibid. **313**, 520 (1993).

[25] R.J. Noble, Nucl. Instrum. Methods **A256**, 427 (1987); R. Blankenbecler and S.D. Drell, Phys. Rev. D **36**, 277 (1987); **37**, 3308 (1988); Phys. Rev. Lett. **61**, 2324 (1988); R. Blankenbecler, S.D. Drell, and N. Kroll, Phys. Rev. D **40**, 2462 (1989); D.V. Schroeder, Ph.D. thesis, SLAC Report No. SLAC-371, 1990.

[26] R. Kleiss and W.J. Stirling, Nucl. Phys. **B262**, 235 (1985); Z. Xu, D.-H. Zhang, and L. Chang, ibid. **B291**, 392 (1987).

[27] See, for example, V. Barger and R. Phillips, Collider Physics (Addison-Wesley, New York, 1987).

[28] O. Nicrosini and L. Trendadue, Nucl. Phys. **B318**, 1 (1989); L. Trentadue et al., in Z Physics at LEP 1, Proceedings of the Workshop, Geneva, Switzerland, 1989, edited by G. Altarelli, R. Kleiss, and C. Verzegnassi (CERN Report No. 89-08, Geneva, 1989), p. 129.

[29] T. Barklow (private communication).

Z. Phys. C **42**, 409 (1989).